ACS APPLIED MATERIALS & INTERFACES

Research Article

www.acsami.org

New Cellulose–Lysine Schiff-Base-Based Sensor–Adsorbent for Mercury Ions

Sapana Kumari and Ghanshyam S. Chauhan*

Department of Chemistry, Himachal Pradesh University, Summer Hill, Shimla, Himachal Pradesh 171005, India

ABSTRACT: Mercury is a highly toxic environmental pollutant; thus, there is an urgent need to develop new materials for its simultaneous detection and removal from water. In the present study, new oxidized cellulose-based materials, including their Schiff bases, were synthesized and investigated as a sensor–adsorbent for simple, rapid, highly selective, and simultaneous detection and removal of mercury [Hg(II)] ions. Cellulose was extracted from the pine needles, etherified, oxidized, and modified to Schiff base by reaction with L-lysine. The well-characterized cellulose Schiff base materials were used as a sensor–adsorbent for Hg(II) from aqueous solution. Hg(II) sensing was analysed with naked-eye detection and fluorescence spectroscopy. Schiff base having a decyl chain, C_{10}–O–cell–HC═N–Lys, was observed to be an efficient adsorbent with a very high maximum adsorption capacity of 258.75 mg g^{-1}. The data were analyzed on the basis of various kinetic and isotherm models, and pseudo-second-order kinetics and Langmuir isotherm were followed for Hg(II) adsorption.

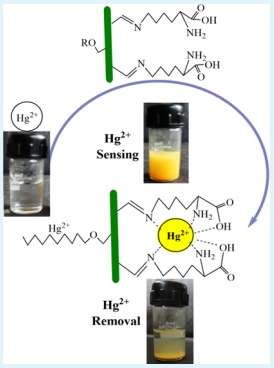

KEYWORDS: *cellulose, Schiff base, Hg(II), fluorescence, adsorption kinetics, adsorption isotherm*

INTRODUCTION

Environmental pollution by toxic heavy metal contamination is one of the major problems to be addressed in the treatment of waste water. Mercury (Hg) is one of the most hazardous elements, and at present, the international community has expressed huge concern regarding its presence in water.[1] Major sources of water pollution by Hg as a contaminant include wood pulping, oil refining, solid waste incineration, coal and gold mining, fossil fuel combustion, rubber processing, and fertilizer industries.[2] Mercury occurs in different forms, such as zero oxidation (Hg^0), mercurous ion (Hg_2^{2+}), and mercuric ion (Hg^{2+}), all of which have very toxic effects, even at a very low concentration. Hg(II) ions can be transformed into the potent neurotoxin methylmercury, which presents a serious environmental concern because of its bioaccumulation and magnification in aquatic food chains. Therefore, it is necessary to develop methods for the highly selective and rapid detection and removal of mercury ions. A variety of sensors, such as functionalized DNA sensors,[3] electrochemical sensors,[4] colorimetric sensors,[5,6] and fluorometric sensors,[7,8] have been reported in the last few years for the detection of Hg ions. Among these, colorimetric and fluorometric sensors are widely studied because of their potential for enabling naked-eye detection in organic media. However, sensing of ions in aqueous medium is thus far a challenge because of their strong hydration.[9] Schiff bases derived from the reaction of aldehyde with amine are important materials in the photometric and fluorescent analysis of metal ions.[10] Schiff bases coordinate metal ions via azomethine nitrogen. Researchers have reported Schiff-base-based materials as metal ion sensors, especially, for Hg(II) detection.[11−14]

Among all of the techniques used for the removal of Hg from water, adsorption is one of the most common and simple methods.[15] In the last few decades, the use of biopolymer-based adsorbents has emerged as one of the most promising alternatives to the conventional heavy metal adsorbents. A variety of biopolymers have been employed for the removal of Hg ions, e.g., chitosan,[16] lignin,[17] pectin,[18] and cellulose.[19,20] Schiff bases of biopolymers are widely reported as effective adsorbents for the removal of metal ions, especially Hg ions.[21] Cellulose-based Schiff bases have also been reported as adsorbents,[22] including for the effective removal of Hg ions.[23] There are many reports on the sensors and adsorbents reported for Hg(II) ions that include nanosize particles. However, there are only a few illustrations in the literature where dual-functional materials have been reported for the simultaneous detection and removal of Hg(II) ions from the aqueous solutions.[24,25] Such materials have huge potential in sensing and purification technologies.

In view of the preceding statement, in the present work, a novel cellulose–lysine–Schiff-base-based sensor–adsorbent was developed using a simple procedure that allows its use for selective mercury detection and removal from water, which is one of the major drawbacks of most of the previously reported Hg sensors and adsorbents. Cellulose is an abundant, biodegradable, and renewable biopolymer that can be chemically modified to have various functional groups that improve its chemical and physical properties for use in a wide range of applications.[26,27] Specific cleavage of the C_2–C_3 bond of anhydroglucose units in the cellulose chain by periodate oxidation generates two aldehyde groups, which can be further derivatized to introduce a variety of functional groups on the

Received: February 8, 2014
Accepted: March 21, 2014
Published: March 21, 2014

   dx.doi.org/10.1021/am500820n | ACS Appl. Mater. Interfaces 2014, 6, 5908–5917

cellulose chain, such as carboxylic acid, hydroxyl, or imines. There are a few reports in the literature where cellulose-based[9] and lysine-based[28,29] Hg(II) sensors have been used. In the present work, a cellulose- and lysine-based Schiff base was designed for the detection and adsorption of Hg(II) from its aqueous solution and a parametric study was designed to understand the kinetics of the adsorption, thereby exploring the potential of the cellulose-based materials in the detection and removal of Hg(II) ions from the aqueous solution. The material reported in the present work was designed with the twin objectives of simultaneous sensing and adsorption of Hg(II). It exhibited rapid and very high removal capacity and naked-eye sensing when investigated within a defined limit, i.e., from 10 ppm and above, i.e., to cover both low and high Hg(II) concentrations. The material reported in this work has high technological potential, because apart from the rapid sensing and scavenging of Hg(II), it is of biological origin and, at the same time, recyclable and reusable.

EXPERIMENTAL SECTION

Materials. All of the chemicals, sodium chlorite (HiMedia, India), butylbromide (SRL, India), sodium hydroxide, isopropanol, octylbromide, and decylbromide (SD Fine Chemicals, Ltd., India), hexyl bromide, mercuric acetate, and sodium periodate (Sigma-Aldrich, Germany), isopropyl alcohol, ethylene glycol, methanol, and L-lysine monohydrochloride (Sarabhai M. Chemicals, India), sodium acetate, 100% (glacial) acetic acid, Michler's thioketone [4,4′-bis(dimethylamino)thiobenzophenone (TMK)], and 1-propanol (Merck, Germany), were of reagent grade and used as received. The concentration of Hg(II) ions was determined with a Photolab 6600 ultraviolet−visible (UV−vis) programmable spectrophotometer, and pH values were measured with a pH meter (Eutech 20).

Synthesis of Cellulose−Lysine-Based Schiff Bases. Cellulose was extracted from powdered oven-dried pine needles of *Pinus wallichiana* using alkali treatment (4 wt % NaOH) at reflux temperature for 4 h to remove lignin and hemicellulose.[30,31] The extracted cellulose was then filtered and washed with distilled water until pH was neutral. Thereafter, it was bleached with 1.7% (w/v) sodium chlorite solution in pH 4 acetic acid buffer (solid/liquid ratio of 1:10, g/mL) at reflux temperature for 4 h. Cellulose was filtered, subsequently washed with distilled water until neutral pH, and dried at room temperature. Extracted cellulose was subjected to etherification before oxidation because, if the reverse is done, a hemiacetal shift may occur in the dialdehyde groups during etherification. Extracted cellulose was treated with 18% NaOH for 2 h at room temperature, precipitated with isopropanol, and then etherified with different alkyl bromides (C_4H_9Br, $C_6H_{13}Br$, $C_8H_{17}Br$, or $C_{10}H_{21}Br$) at 60 °C for 6 h. The products were extracted with methanol and dried at room temperature. Etherified cellulose (1.0 g) was subjected to oxidation at the C_2-C_3 position with $NaIO_4$ (1.65 g) at room temperature for 72 h in the dark, and thereafter, the remaining $NaIO_4$ was neutralized with an excess of ethylene glycol.[32] The product (R−O−cell−HC═O) was filtered and washed with ethanol and water. Etherified oxidized cellulose (R−O−cell-HC═O) was then treated with L-lysine monohydrochloride in pH 7.2 phosphate buffer at 37 °C for 5 h.[33] The product (R−O−cell−HC═N−Lys, where R = butyl, hexyl, octyl, or decyl) was filtered, washed with phosphate buffer (pH 7.2), and dried at room temperature.

Determination of the Aldehyde Content. The degree of oxidization of cellulose was evaluated by the determination of the aldehyde content.[32,34] Dialdehyde cellulose (R−O−cell−HC═O, DAC) was converted to oxime by Schiff's base reaction with hydroxylamine hydrochloride. A total of 0.1 g of DAC was suspended in 30 mL of distilled water, and the pH was adjusted to 4.5 with HCl and NaOH. Hydroxylamine hydrochloride solution (0.43 g in 20 mL of water at pH 4.5) was added to the DAC suspension. The mixture was stirred for 4 h in a water bath at 40 °C, and then released HCl was titrated with 0.1 N NaOH. The consumption of NaOH solution was recorded as V_c (L). The consumption of NaOH solution, V_b (L), for etherified cellulose at pH 4.5 was used as a blank. The aldehyde content (AC) in R−O−cell−HC═O was calculated by

$$\mathrm{AC}\ (\%) = \frac{M_{\mathrm{NaOH}}(V_c - V_b)}{m/M_w} \times 100 \quad (1)$$

where M_{NaOH} is 0.1 N, m is the dry weight of the DAC sample (g), and M_w is approximately the molecular weight of the repeating unit in R−O−cell−HC═O.

Characterization of Cellulose−Lysine−Schiff Bases (R−O−Cell−HC═N−Lys). The synthesized cellulose−lysine-based Schiff bases were characterized using Fourier transform infrared (FTIR) spectroscopy, scanning electron microscopy (SEM), X-ray diffraction (XRD), and energy-dispersive X-ray analysis (EDAX) to obtain the evidence of modification. The FTIR spectrum was recorded on a PerkinElmer FTIR spectrophotometer between 400 and 4000 cm^{-1} using the KBr pellet technique. SEM−EDAX was recorded on SEM Quanta 250 D9393 for determination of surface morphological changes and elemental analysis. XRD patterns were recorded on a Philips PAN Analytical XPERT-PRO X-ray diffractometer using a wavelength of 1.540 60 Å (Cu Kα radiation), with the diffraction angle 2θ varied from 10° to 70°. ^{13}C nuclear magnetic resonance (NMR) was recorded on a Bruker 300 MHz solid-state NMR spectrometer.

Metal Ion Detection and Removal from Aqueous Solution Using Cellulose−Lysine−Schiff Bases (R−O−Cell−HC═N−Lys). *Metal Ion Detection.* A total of 10 mg of synthesized Schiff base was added to 10 mL (100 ppm solution) of Hg^{2+}, Fe^{2+}, Zn^{2+}, Cd^{2+}, Pb^{2+}, or Sr^{2+} ions for sensing of the color change by the naked eye and fluorescence spectroscopy using a LS50 luminescence spectrophotometer (PerkinElmer). The photographs were taken with a digital camera.

Hg(II) Ion Removal from Aqueous Solution. The ion solutions were prepared by dissolving mercuric acetate [$Hg(CH_3COO)_2$] in deionized water. The ion removal study was carried out on the above synthesized Schiff bases using 0.01 g of polymer in 10.0 mL of Hg(II) solution (100 ppm). After specific time intervals (10−180 min), solution aliquots were withdrawn and the concentration of the remaining ions was determined at 560 nm with a Photolab 6600 UV−vis spectrophotometer using Michler's thioketone (TMK) reagent to evaluate the best performing adsorbent and equilibrium adsorption time for further adsorption experiments.[35] In view of the higher efficiency of C_{10}−O−cell−HC═N−Lys than the other adsorbents, it was selected for the optimization of various adsorption parameters, such as the temperature, pH, and initial concentration of ion solutions. The effects of the temperature (20−60 °C), pH (2.0−8.0), and initial Hg(II) ion concentration (10−200 ppm) were studied at the optimized time.

The maximum removal capacity (MRC) of the polymer was determined by the repeated treatments of the same sample using 150 ppm of metal ions at the optimized conditions obtained for the maximum ion uptake. The reusability studies were also carried out to assess the regeneration of the adsorbent by stripping off the adsorbed ions with 0.5 N HCl. The sorption results were evaluated with the following expressions:

$$\text{adsorption capacity } (q)\ (\mathrm{mg/g}) = \frac{(C_o - C_t)V}{m} \quad (2)$$

where q is the amount of ions adsorbed onto a unit dry mass of the polymer (mg/g), C_o and C_t are the initial and residual concentrations (mg/L) of metal ions after time t in solution, respectively, V is the volume of the aqueous phase (L), and m is the weight of the dry polymer (g).

Kinetics of Ion Adsorption. The efficiency of the absorbent was evaluated from pseudo-first-order, pseudo-second-order, and Elovich kinetic models to understand the mechanism of adsorption on C_{10}−O−cell−HC═N−Lys. The rate constant of adsorption was determined from the pseudo-first-order equation, which is generally expressed as[36]

$$\ln(q_e - q_t) = \ln q_e - k_1 t \quad (3)$$

Scheme 1. Synthesis of Cellulose−Lysine−Schiff Base

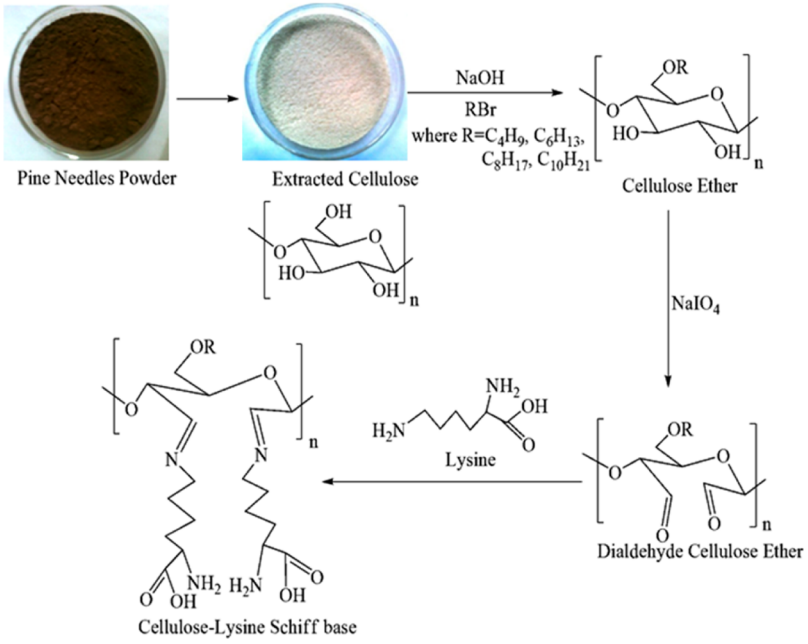

where q_e and q_t are the adsorption capacities (mg/g) at equilibrium and time t, respectively, and k_1 is the rate constant for pseudo-first-order adsorption. From the plots of $\ln(q_e - q_t)$ versus t, the values of k_1 and q_e were determined. The linear form of the pseudo-second-order kinetic model is expressed as[37]

$$\frac{t}{q_t} = \frac{1}{k_2 q_e^{\,2}} + \left(\frac{1}{q_e}\right)t \tag{4}$$

where k_2 is the rate constant for second-order adsorption (g mg^{-1} min^{-1}) and is determined from the linear plot of t/q_t versus t.

The linear form of the Elovich equation is given as[38]

$$q_t = \frac{1}{\beta}\ln(\alpha\beta) + \frac{1}{\beta}\ln t \tag{5}$$

Constants α and β were calculated from the slope and intercept of the plot q_t versus ln t. The Langmuir and Freundlich adsorption isotherms were used to describe the adsorption equilibrium over the entire concentration range studied. The saturated monolayer Langmuir isotherm[39] can be represented as

$$q_e = \frac{q_m b C_e}{1 + bC_e} \tag{6}$$

The constants q_m and b are characteristics of the Langmuir equation and can be determined from its linear form, represented by[40]

$$\frac{C_e}{q_e} = \frac{C_e}{q_m} + \frac{1}{bq_m} \tag{7}$$

or alternatively

$$\frac{1}{q_e} = \frac{1}{bq_m}\frac{1}{C_e} + \frac{1}{q_m} \tag{8}$$

where C_e (mg/L) is the equilibrium metal ion concentration, q_e (mg/g) is the amount of Hg(II) adsorbed on the adsorbent at equilibrium, and the parameters q_m (mg/g) and b (L/mg) are the Langmuir constants that relate q_e for a complete monolayer and energy of adsorption, respectively. These constants can be calculated from the linear plot of C_e/q_e versus C_e or $1/q_e$ versus $1/C_e$. The essential characteristics of the Langmuir isotherm can be expressed in terms of a dimensionless constant called the equilibrium parameter (R_L), which is defined as follows:

$$R_L = 1/(1 + bC_o) \tag{9}$$

where C_o is the initial Hg(II) ion concentration (mg/L). The R_L value indicates the shape and favorability of the adsorption isotherm. R_L values between 0 and 1 indicate a favorable adsorption system.

The Freundlich isotherm[41] is expressed by the following equation:

$$q_e = K_F C_e^{\,1/n} \tag{10}$$

The linear logarithmic form of the Freundlich equation is as follows:

$$\ln q_e = \ln K_F + \frac{1}{n}\ln C_e \tag{11}$$

where K_F (mg/g) and $1/n$ indicate adsorption capacity and adsorption intensity, respectively. The plot of ln q_e versus ln C_e gives a straight line with a slope of $1/n$ and an intercept of ln K_F.

Thermodynamic Study. Thermodynamics for the adsorption of Hg(II) was investigated in the temperature range of 20−60 °C according to the van't Hoff equation[21]

$$\ln K_c = \frac{\Delta S^\circ}{R} - \frac{\Delta H^\circ}{RT} \tag{12}$$

where ΔH°, ΔS°, and R represent enthalpy, entropy, and the gas constant (8.314 J mol^{-1} K^{-1}), respectively. The values of ΔH° and ΔS° are calculated from the slope and intercept of the linear plot between ln K_c versus $1/T$. The thermodynamic equilibrium constant, K_c, for the adsorption of Hg(II) was calculated using the equation

$$K_c = \frac{X_e}{C_i - X_e} \tag{13}$$

where X_e is the concentration of solute adsorbed on the adsorbent at equilibrium and C_i is the initial ion concentration.

The standard free energy change is calculated as

$$\Delta G^\circ = -RT \ln K_c \tag{14}$$

RESULTS AND DISCUSSION

Synthesis and Characterization of Cellulose−Lysine−Schiff Bases. Periodate oxidation of cellulose generates (−CHO) functional groups that give Schiff bases upon reaction

with amines. In the present work, the extracted cellulose was first etherified for ensuring stability of the final product and, subsequently, oxidized to dialdehyde (R−O−cell−HC═O) using $NaIO_4$. The latter was functionalized to the corresponding Schiff base (R−O−cell−HC═N−Lys) by reaction with lysine as per Scheme 1.

The aldehyde contents of 48, 51.8, 51.2, 59.8, and 62.9% were calculated for dialdehyde celluloses cell−HC═O, C_4−O−cell−HC═O, C_6−O−cell−HC═O, C_8−O−cell−HC═O, and C_{10}−O−cell−HC═O, respectively. FTIR spectra confirming the extraction of cellulose from pine needles as peaks, which were observed in the FTIR spectra of pine needles at 1736 cm^{-1} (acetyl and ester groups in hemicellulose or carboxylic acid groups in the ferulic and *p*-coumeric components of lignin), 1509 cm^{-1} (aromatic −C═C stretching in lignin), and 1250 cm^{-1} (−C−O−C stretching in lignin), were not present in the spectrum of the extracted cellulose (Figure 1). The FTIR

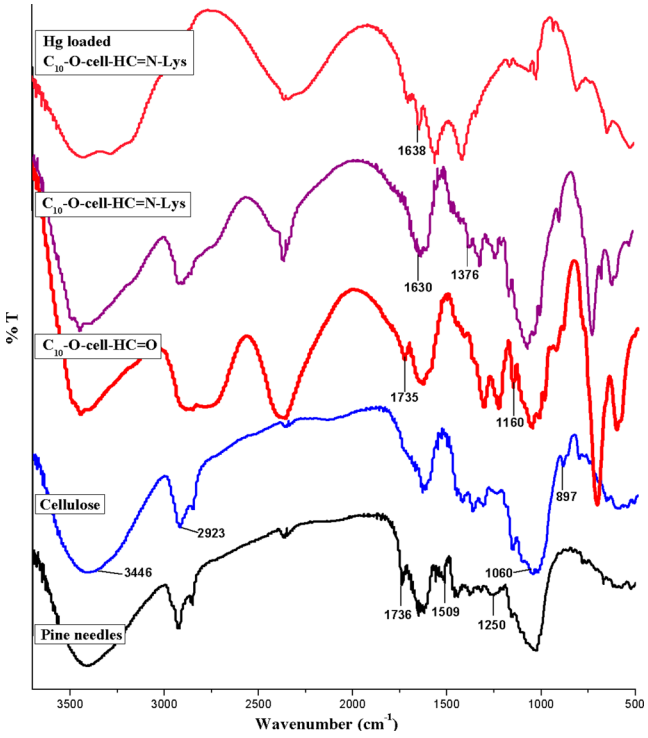

Figure 1. FTIR spectra of pine needles, extracted cellulose, oxidized decyl cellulose [C_{10}−O−cell−HC═O], Schiff base [C_{10}−O−cell−HC═N−Lys], and Hg(II)-loaded C_{10}−O−cell−HC═N−Lys.

of extracted cellulose showed peaks at 3446 cm^{-1} (−O−H stretching), 2923 cm^{-1} (−C−H stretching), 1060 cm^{-1} (−C−O−C pyranose ring skeletal vibration), and 897 cm^{-1} (*β*-glycosidic linkages). The FTIR spectrum of etherified oxidized cellulose (C_{10}−O−cell−CH═O) showed peaks at 1160 cm^{-1} (−C−O stretching of the −C−O−C group), 1735 cm^{-1} (−C═O stretching), and 2891 cm^{-1} (−C−H stretching in aldehyde). The synthesis of Schiff base (C_{10}−O−cell−HC═N−Lys) was indicated by the appearance of peaks at 1630 cm^{-1} (−C═N, characteristic of imine) and 1376 cm^{-1} ($-COO^-$ sym stretching).

The XRD patterns reveal a high crystalline nature for the extracted cellulose with a major intensity peak located at a 2*θ* value of around 22.78°, which is related to the crystalline structure of cellulose (Figure 2).

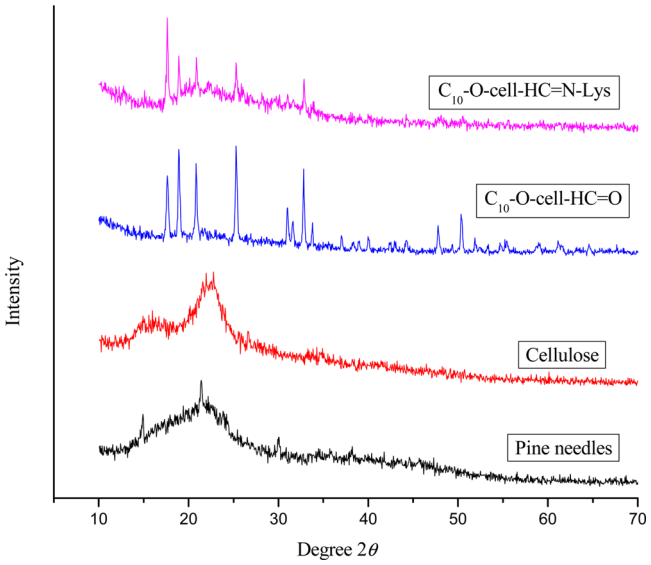

Figure 2. XRD pattern of pine needles, extracted cellulose, C_{10}−O−cell−HC═O, and C_{10}−O−cell−HC═N−Lys.

The crystallinity indices of raw pine needle powder and extracted cellulose were found to be 67.15 and 85.54%, respectively. The XRD pattern of the native cellulose has peaks at 2*θ*, with intensity given within the parentheses, of 14.37° (23.06), 16.68° (33.69), and 22.78° (150.27), corresponding to (110), (11$\bar{0}$), and (200) crystal planes of cellulose, respectively.[42] The sharp peaks in the XRD patterns of C_{10}−O−cell−CHO and C_{10}−O−cell−HC═N−Lys indicate their crystalline nature. These peaks are at 2*θ* of 17.63° (200.6), 18.91° (284.5), 20.83° (212.5), and 25.28° (292.54) and 17.62° (187.52), 18.92° (104.30), 20.76° (35.43), and 25.29° (75.22) for C_{10}−O−cell−HC═O and C_{10}−O−cell−HC═N−Lys, respectively. The crystalline nature of the periodate-oxidized cellulose has been reported.[43,44] In the present case, it is reasonable to assume that aldehyde groups of hydrophobically modified C_{10}−O−cell−CHO may associate to generate a well-packed structure, hence, the crystalline nature. The same becomes disrupted on Schiff base formation with lysine, resulting in the lower crystallinity of C_{10}−O−cell−HC═N−Lys.

From SEM analysis (Figure 3), it was observed that the cellulose fibers loosen and become separated into individual fibers in the case of extracted cellulose after chemical treatment of pine needles. The surfaces of C_{10}−O−cell−HC═O and C_{10}−O−cell−HC═N−Lys look crystalline compared to the extracted cellulose because the cellulose structure loosens as a result of the introduction of hydrophobic alkyl chains via the etherification reaction. The Schiff base synthesis is confirmed by the presence of a high N content of 7.61 wt % in the EDAX of C_{10}−O−cell−HC═N−Lys (Figure 4B).

The solid-state ^{13}C NMR (Figure 5) studies further confirmed the extraction of cellulose and its derivatization. The spectrum of the extracted cellulose has dominate peaks at 62.42 and 65.08 ppm (C-6), 72.01, 74.79, and 79.44 ppm (C-2, C-3, and C-5), 83.66 and 88.74 ppm (C-4), and 104.89 ppm (C-1), respectively. Modification of cellulose through etherification with decyl bromide is confirmed by the shifting of peaks present in cellulose, along with the appearance of peaks as a result of the $C_{10}H_{21}$ group mainly in the region of 24.01−32.49 ppm.

dx.doi.org/10.1021/am500820n | ACS Appl. Mater. Interfaces 2014, 6, 5908−5917

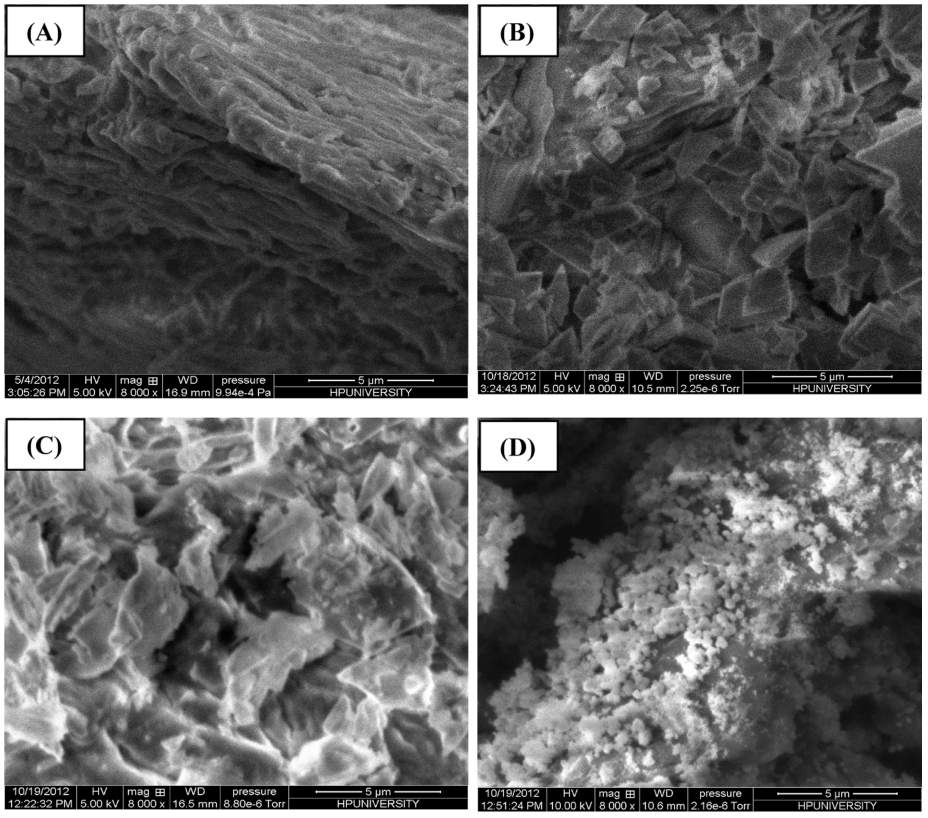

Figure 3. SEM images of (A) extracted cellulose, (B) C_{10}–O–cell–HC═O, (C) C_{10}–O–cell–HC═N–Lys, and (D) Hg(II)-loaded C_{10}–O–cell–HC═N–Lys.

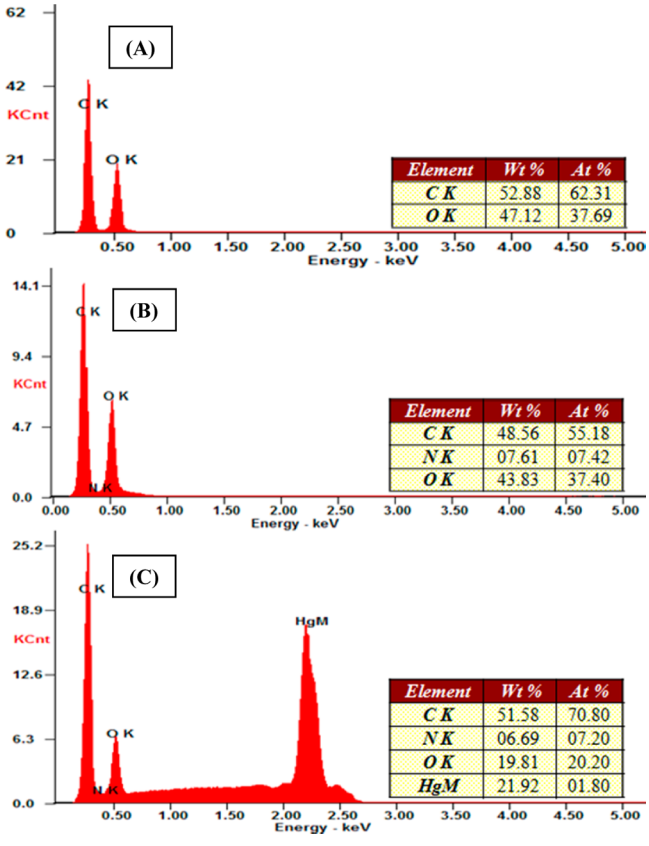

Figure 4. EDAX of (A) C_{10}–O–cell–HC═O, (B) C_{10}–O–cell–HC═N–Lys, and (C) Hg(II)-loaded C_{10}–O–cell–HC═N–Lys.

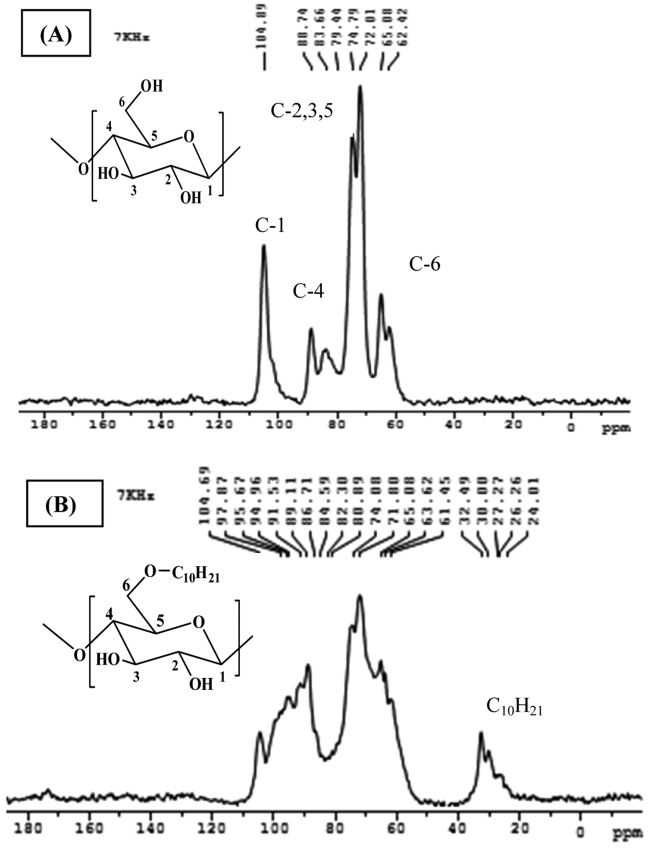

Figure 5. Solid-state ^{13}C NMR of (A) extracted cellulose and (B) decyl cellulose.

dx.doi.org/10.1021/am500820n | ACS Appl. Mater. Interfaces 2014, 6, 5908–5917

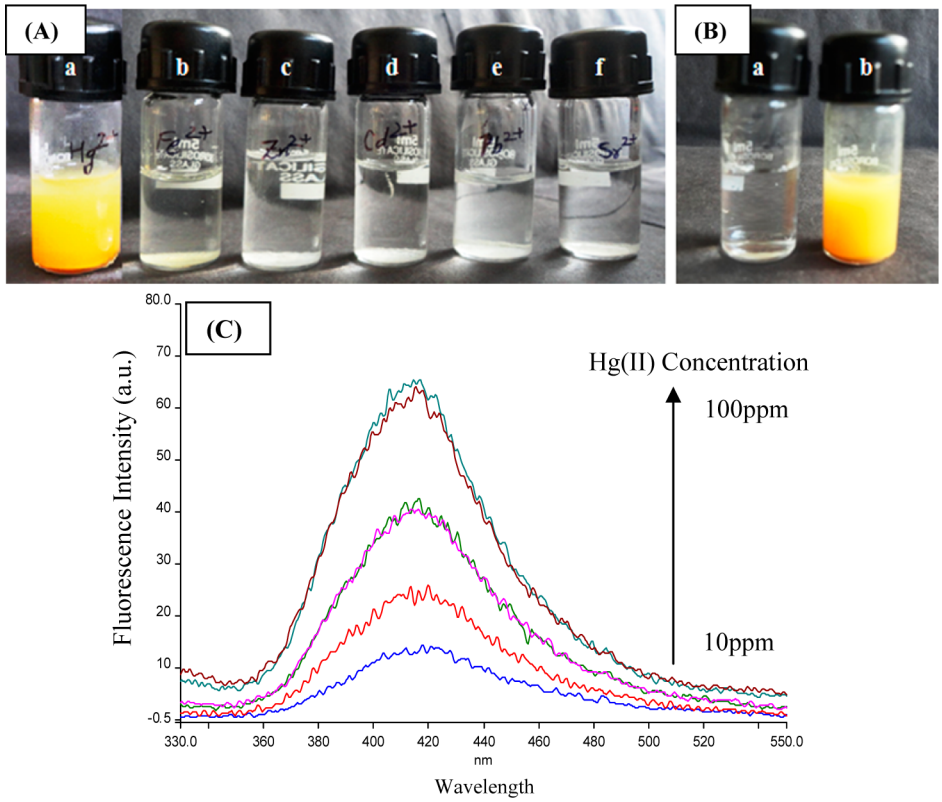

Figure 6. (A) Color changes of metal ion solution (100 ppm): (a–f) Hg^{2+}, Fe^{2+}, Zn^{2+}, Cd^{2+}, Pb^{2+}, and Sr^{2+} after the addition of 10 mg of synthesized Schiff base. (B) Color change of Hg(II) solution (a) before and (b) after the addition of synthesized Schiff base. (C) Fluorescence spectra of different concentrations of Hg(II) (10, 20, 40, 50, 75 and 100 ppm) after the addition of 10 mg of Schiff base (λ_{ex} = 300 nm).

Hg(II) Ion Sensing. Among the metal ions studied for the interaction with the synthesized Schiff bases, the color change was visualized by the naked eye only with Hg(II) ions (Figure 6A).

After the addition of C_{10}–O–cell–HC═N–Lys, the colorless Hg(II) solution changed into yellow solution because of the formation of a colored complex between the Schiff base and Hg(II) ions (Figure 6B). The complex was formed within <30 s, and the lowest concentration limit of Hg(II) ion for visual detection was observed from 10 ppm onwards, with a sharp increase in intensity observed at 40 ppm. The fluorescence spectra were obtained by excitation of the Hg solution after adding synthesized Schiff base at 300 nm, and emission spectra were obtained at 415 nm. Large fluorescence enhancement was shown after the addition of Schiff base on increase of the concentration of Hg(II) solution. With the increase in the concentration of Hg(II) ions from 10 to 100 ppm, the fluorescence intensity was found to increase from 12.79 to 62.18 au (Figure 6C). The Hg(II) ions and sensor form a complex that undergoes π–π^* electronic transitions. λ_{max} was observed at 295 nm in the UV spectrum. The large red shift to the yellow color on the interaction of the sensor and Hg(II) ions results from the formation of the ligand–metal charge transfer complex.

Parametric Studies of the Adsorption of Hg(II) Ions. The effect of the different adsorption parameters, such as the contact time, temperature, pH, and Hg(II) concentration, was studied to evaluate the best conditions for the maximum ion removal from its aqueous solutions. Variation of time was studied from 10 to 180 min in batch experiments with 100 mg L^{-1} Hg(II) at pH 4.4 at 30 °C. Adsorption capacity (q) was observed to increase with time, and the equilibrium was attained after 60 min (Figure 7A). Of all of the adsorbents used, C_{10}–O–cell–HC═N–Lys exhibited the maximum adsorption capacity of 50.6 mg/g. Hence, it was selected for further studies. Temperature variation had a positive effect on the q values. These increased sharply from 40.2 to 75.2 mg/g with the temperature variation from 20 to 50 °C, and thereafter, equilibrium was attained with the further increase in the temperature (Figure 7B). With an increase in the temperature, the polymer structure opens and more active sites become accessible to the metal ions; hence, adsorption capacity was observed to increase.[45]

Adsorption of Hg(II) ions is strongly dependent upon pH. The effect of pH variation on the adsorption of Hg(II) was studied in the pH range of 1.0–8.0. As seen in Figure 7B, adsorption was observed to increase with the increase in pH and then reached almost a plateau at pH 5.0. The adsorption capacity increased from 27.3 to 84.2 mg/g with the increase in pH from 2 to 5. At lower pH, the protonation of active sites, imine groups, on the adsorbent surface takes place, resulting in the electrostatic repulsions between the metal cations and the protonated groups, and prevents the adsorption of the metal ions, hence resulting in lower Hg(II) ion uptake with a low q value. At higher pH, free imine groups are available on the adsorbent for ion adsorption; hence, q values increased with pH,[46,47] but the precipitation of Hg as $Hg(OH)_2$ takes place at pH ≥ 6. Hence, pH 5.0 was selected as the optimum pH for further studies.[38] The effect of the initial concentration of Hg(II) on the adsorption capacity is shown in Figure 7C. Hg(II) adsorption capacity of the adsorbents increased initially from 1.135 to 121.2 mg/g with the increasing Hg(II) concentration (10–150 ppm), and then equilibrium was reached.

For reusability studies, Hg(II)-loaded adsorbent was regenerated by treatment with 0.5 N HCl solution for 5 min.

dx.doi.org/10.1021/am500820n | ACS Appl. Mater. Interfaces 2014, 6, 5908–5917

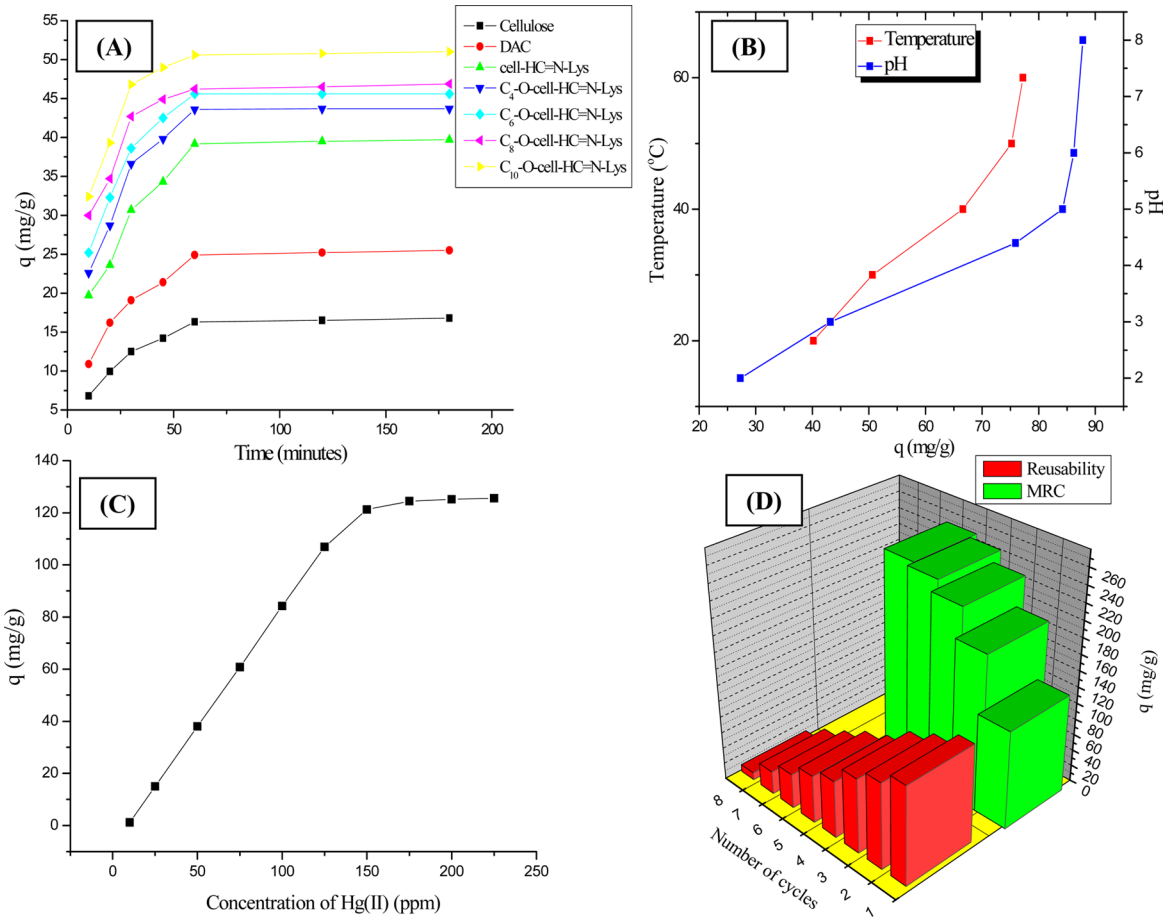

Figure 7. (A) Hg(II) ion adsorption onto different synthesized polymers with respect to time variation at pH 4.4, T of 30 °C, and Hg(II) ion concentration of 100 ppm. (B) Hg(II) ion adsorption onto C_{10}−O−cell−HC═N−Lys with respect to the temperature and pH. (C) Hg(II) ion concentration variation. (D) Reusability and MRC of C_{10}−O−cell−HC═N−Lys for Hg(II) ion adsorption at optimized conditions.

Table 1. Parameters of the Kinetic Models for Adsorption of Hg(II) on C_{10}−O−Cell−HC═N−Lys

pseudo-first-order			pseudo-second-order			Elovich equation		
k_1 (min^{-1})	q_e (mg/g)	R^2	k_2 (g mg^{-1} min^{-1})	q_e (mg/g)	R^2	α (mg g^{-1} min^{-1})	β (g/mg)	R^2
7.25×10^{-2}	48.10	0.984	3.29×10^{-3}	55.04	0.999	103.52	0.14	0.784

The regenerated hybrid materials were reused for 8 repeat cycles, and the results are illustrated in Figure 7D. Schiff bases are not generally stable and lack reusability. However, in the present case, the short treatment time and nature of the material used ensure it stability. It is effectively reusable for many cycles because the presence of bulky hydrophobic alkyl groups in the surroundings of the −C═N− bond protect the imine bond against hydrolysis and increase its stability. The efficacy of the material was also obtained from the high MRC of 258.75 mg g^{-1} that was obtained after 5 repeat cycles when the same sample was used time and time again (Figure 7D). The obtained values are close to the adsorption capacity of 269.5 mg g^{-1} calculated from the Langmuir isotherm.

Kinetics, Isotherm, and Mechanism of Adsorption. Three kinetic models, pseudo-first-order, pseudo-second-order, and Elovich equation, were applied to examine the adsorption kinetics. Various parameters calculated from the plots of kinetic models are represented in Table 1.

The pseudo-second-order model best-fitted the experimental data with a correlation coefficient value (R^2 = 0.999) close to 1, as compared to the pseudo-first-order model (R^2 = 0.984) and the Elovich model (R^2 = 0.784). Moreover, the values of q calculated from the pseudo-second-order model are closer to the experimental values (Figure 8A).

Various parameters calculated from the Langmuir and Freundlich isotherm plots are given in Table 2.

The value of R^2 was found to be higher for the Langmuir isotherm (0.982) compared to the Freundlich isotherm (0.975). In addition, the values of q calculated from the Langmuir isotherm are quite close to the experimental values (Figure 8B). The value R_L = 0.752 lies between 0 and 1, indicating a favorable adsorption process. Thermodynamic parameters $\Delta G°$, $\Delta H°$, and $\Delta S°$ values were evaluated from the slope and intercept of the van't Hoff plot (Figure 8C) and are presented in Table 3.

With increase in the temperature from 20 to 60 °C, the magnitude of free energy change ($\Delta G°$) shifted to a high negative value, suggesting that adsorption was rapid and spontaneous. The positive value of $\Delta H°$ confirmed the endothermic nature of adsorption and high temperature preferable for adsorption. The positive value of $\Delta S°$ suggested an increase in randomness at the solid−solution interface during the adsorption of Hg(II) on the polymer.

dx.doi.org/10.1021/am500820n | ACS Appl. Mater. Interfaces 2014, 6, 5908−5917

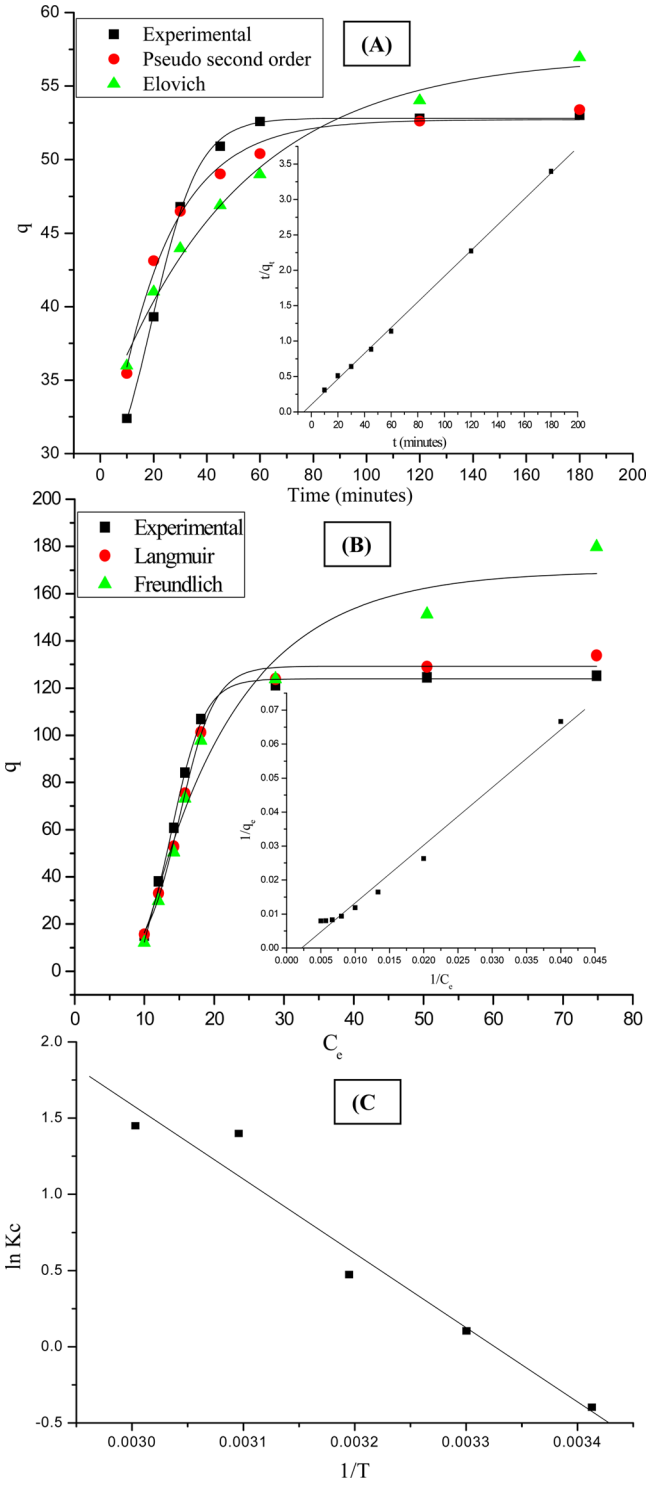

Figure 8. (A) Comparison of different kinetic models for the adsorption of Hg(II) ions by C_{10}−O−cell−HC═N−Lys. (Inset) Linear fit of the pseudo-second-order model. (B) Comparison of different isotherms for the adsorption of Hg(II) ions by C_{10}−O−cell−HC═N−Lys. (Inset) Linear fit of the Langmuir plot. (C) van't Hoff plot for Hg(II) removal by C_{10}−O−cell−HC═N−Lys.

Table 3. Thermodynamic Parameters for Adsorption of Hg(II) by C_{10}−O−Cell−HC═N−Lys

temperature (K)	$-\Delta G°$ (kJ/mol)	$\Delta H°$ (kJ/mol)	$\Delta S°$ (J mol^{-1} K^{-1})
293	0.105	40.519	138.65
303	1.491		
313	2.878		
323	4.264		
333	5.651		

Evidence to support the adsorption of Hg(II) was obtained from the FTIR spectrum of the Hg(II)-loaded C_{10}−O−cell−HC═N−Lys. The adsorption of Hg(II) on the polymer is indicated by the shifting of the position with the change in intensity of some basic peaks and the presence of the additional peaks in the FTIR spectrum (Figure 1). The shift in the characteristic peak of −C═N from 1630 to 1638 cm^{-1} indicates that the −C═N bond is the main adsorption site for Hg(II) adsorption. In addition, the peaks corresponding to amino acid moiety shift to a higher wave number after Hg(II) adsorption, indicating that these groups also take part in adsorption. Similarly, the SEM image of Hg(II)-loaded C_{10}−O−cell−HC═N−Lys (Figure 3D) has different surface morphologies than its precursor C_{10}−O−cell−HC═N−Lys (Figure 3C). Furthermore, the EDAX of Hg(II)-loaded C_{10}−O−cell−HC═N−Lys shows the presence of a peak corresponding to Hg in the spectrum (Figure 4C), supporting the adsorption of Hg(II) ions onto the adsorbent.

CONCLUSION

A new cellulose−lysine Schiff-base-based sensor−adsorbent from biowaste was designed to be effective sensors and adsorbents for adsorption of Hg(II) from its aqueous solutions. Hg(II) sensing was studied from the lower limit of 10 ppm, and adsorption was found to be effective at pH 5.0 and 50 °C with 150 ppm Hg(II) ion solution for 1 h. The adsorption follows pseudo-second-order kinetics and Langmuir isotherm and was observed to be a feasible, spontaneous, and endothermic adsorption process. The candidate material exhibited a very high maximum removal capacity and good reusability up to 8 cycles, and therefore, these Schiff base materials behave as good candidates for Hg(II) ion detection and removal in water purification technologies.

AUTHOR INFORMATION

Corresponding Author

*Telephone: +911772830944. Fax: +911772830775. E-mail: ghanshyam_in2000@yahoo.com and/or ghanshyamschauhan@gmail.com.

Notes

The authors declare no competing financial interest.

ACKNOWLEDGMENTS

The authors acknowledge the financial support by University Grants Commission (UGC), New Delhi, India, in the form of a UGC−Basic Scientific Research (BSR) scholarship and facilities

Table 2. Isotherm Models for Adsorption of Hg(II) on C_{10}−O−Cell−HC═N−Lys

	Langmuir			Freundlich		
q_m (mg/g)	b (L/mg)	R_L	R^2	K_F (mg/g)	n	R^2
269.5	2.2 × 10^{-3}	0.752	0.982	5.32	0.772	0.975

under Special Assistance Programme (SAP)−Departmental Research Support II (DRS II).

REFERENCES

(1) United Nations Environment Programme (UNEP). *Global Mercury Assessment 2013: Sources, Emissions, Releases and Environmental Transport*; UNEP: Geneva, Switzerland, 2013.
(2) Nolan, E. M.; Lippard, S. J. Tools and tactics for the optical detection of mercuric ion. *Chem. Rev.* **2008**, *108*, 3443−3480.
(3) Guo, Z.; Duan, J.; Yang, F.; Li, M.; Hao, T.; Wang, S.; Wei, D. A test strip platform based on DNA-functionalized gold nanoparticles for on-site detection of mercury(II) ions. *Talanta* **2012**, *93*, 49−54.
(4) Gong, J.; Zhou, T.; Song, D.; Zhang, L.; Hu, X. Stripping voltammetric detection of mercury(II) based on a bimetallic Au−Pt inorganic−organic hybrid nanocomposite modified glassy carbon electrode. *Anal. Chem.* **2010**, *82*, 567−573.
(5) Kim, Y. R.; Mahajan, R. K.; Kim, J. S.; Kim, H. Highly sensitive gold nanoparticle-based colorimetric sensing of mercury(II) through simple ligand exchange reaction in aqueous media. *ACS Appl. Mater. Interfaces* **2010**, *2*, 292−295.
(6) Chen, L.; Fu, X.; Lu, W.; Chen, L. Highly sensitive and selective colorimetric sensing of Hg^{2+} based on the morphology transition of silver nanoprisms. *ACS Appl. Mater. Interfaces* **2013**, *5*, 284−290.
(7) Li, H.; Zhai, J.; Tian, J.; Luo, Y.; Sun, X. Carbon nanoparticle for highly sensitive and selective fluorescent detection of mercury(II) ion in aqueous solution. *Biosens. Bioelectron.* **2011**, *26*, 4656−4660.
(8) Lu, X.; Guo, Z.; Feng, M.; Zhu, W. Sensing performance enhancement via acetate-mediated N-acylation of thiourea derivatives: A novel fluorescent turn-on Hg^{2+} chemodosimeter. *ACS Appl. Mater. Interfaces* **2012**, *4*, 3657−3662.
(9) Diez-Gil, C.; Caballero, A.; Ratera, I.; Tarraga, A.; Molina, P.; Veciana, J. Naked-eye and selective detection of mercury(II) ions in mixed aqueous media using a cellulose-based support. *Sensors* **2007**, *7*, 3481−3488.
(10) Ye, J.; Xiong, J.; Sun, R. The fluorescence property of Schiff's bases of carboxymethyl cellulose. *Carbohydr. Polym.* **2012**, *88*, 1420−1424.
(11) Alizadeh, K.; Parooi, R.; Hashemi, P.; Rezaei, B.; Ganjali, M. R. A new Schiff's base ligand immobilized agarose membrane optical sensor for selective monitoring of mercury ion. *J. Hazard. Mater.* **2011**, *186*, 1794−1800.
(12) Mashhadizadeh, M. H.; Sheikhshoaie, I. Mercury(II) ion-selective polymeric membrane sensor based on a recently synthesized Schiff base. *Talanta* **2003**, *60*, 73−80.
(13) Wang, J.; Huang, L.; Xue, M.; Liu, L.; Wang, Y.; Gao, L.; Zhu, J.; Zou, Z. Developing a novel fluorescence chemosensor by self-assembly of bis-Schiff base within the channel of mesoporous SBA-15 for sensitive detecting of Hg^{2+} ions. *Appl. Surf. Sci.* **2008**, *254*, 5329−5335.
(14) Quang, D. T.; Wu, J. S.; Luyen, N. D.; Duong, T.; Dan, N. D.; Bao, N. C.; Quy, P. T. Rhodamine-derived Schiff base for the selective determination of mercuric ions in water media. *Spectrochim. Acta, Part A* **2011**, *78*, 753−756.
(15) Aguado, J.; Arsuaga, J. M.; Arencibia, A. Adsorption of aqueous mercury(II) on propylthiol-functionalized mesoporous silica obtained by co-condensation. *Ind. Eng. Chem. Res.* **2005**, *44*, 3665−3671.
(16) Shafaei, A.; Ashtiani, F. Z.; Kaghazchi, T. Equilibrium studies of the sorption of Hg(II) ions onto chitosan. *Chem. Eng. J.* **2007**, *133*, 311−316.
(17) Lv, J.; Luo, L.; Zhang, J.; Christie, P.; Zhang, S. Adsorption of mercury on lignin: Combined surface complexation modeling and X-ray absorption spectroscopy studies. *Environ. Pollut.* **2012**, *162*, 255−261.
(18) Cataldo, S.; Gianguzza, A.; Pettignano, A.; Villaescusa, I. Mercury(II) removal from aqueous solution by sorption onto alginate, pectate and polygalacturonate calcium gel beads. A kinetic and speciation based equilibrium study. *React. Funct. Polym.* **2013**, *73*, 207−217.
(19) Takagai, Y.; Shibata, A.; Kiyokawa, S.; Takase, T. Synthesis and evaluation of different thio-modified cellulose resins for the removal of mercury(II) ion from highly acidic aqueous solutions. *J. Colloid Interface Sci.* **2011**, *353*, 593−597.
(20) Donia, A. M.; Atia, A. A.; Abouzayed, F. I. Preparation and characterization of nano-magnetic cellulose with fast kinetic properties towards the adsorption of some metal ions. *Chem. Eng. J.* **2012**, *191*, 22−30.
(21) Monier, M. Adsorption of Hg^{2+}, Cu^{2+} and Zn^{2+} ions from aqueous solution using formaldehyde cross-linked modified chitosan−thioglyceraldehyde Schiff's base. *Int. J. Biol. Macromol.* **2012**, *50*, 773−781.
(22) da Silva Filho, E. C.; de Melo, J. C. P.; da Fonseca, M. G.; Airoldi, C. Cation removal using cellulose chemically modified by a Schiff base procedure applying green principles. *J. Colloid Interface Sci.* **2009**, *340*, 8−15.
(23) Navarro, R. R.; Sumi, K.; Fujii, N.; Matsumura, M. Mercury removal from wastewater using porous cellulose carrier modified with polyethyleneimine. *Water Res.* **1996**, *30*, 2488−2494.
(24) Dave, N.; Chan, M. Y.; Huang, P. J.; Smith, B. D.; Liu, J. Regenerable DNA-functionalized hydrogels for ultrasensitive, instrument-free mercury(II) detection and removal in water. *J. Am. Chem. Soc.* **2010**, *132*, 12668−12673.
(25) Wang, C.; Tao, S.; Wei, W.; Meng, C.; Liu, F.; Han, M. Multifunctional mesoporous material for detection, adsorption and removal of Hg^{2+} in aqueous solution. *J. Mater. Chem.* **2010**, *20*, 4635−4641.
(26) Chauhan, G. S.; Guleria, L.; Sharma, R. Synthesis, characterization and metal ion sorption studies of graft copolymers of cellulose with glycidyl methacrylate and some comonomers. *Cellulose* **2005**, *12*, 97−110.
(27) Chauhan, G. S.; Singh, B.; Chauhan, S.; Verma, M.; Mahajan, S. Sorption of some metal ions on cellulosic-based hydrogels. *Desalination* **2005**, *181*, 217−224.
(28) Chen, L.; Yang, L.; Li, H.; Gao, Y.; Deng, D.; Wu, Y.; Ma, L. J. Tridentate lysine-based fluorescent sensor for Hg(II) in aqueous solution. *Inorg. Chem.* **2011**, *50*, 10028−10032.
(29) Sener, G.; Uzun, L.; Denizli, A. Lysine-promoted colorimetric response of gold nanoparticles: A simple assay for ultrasensitive mercury(II) detection. *Anal. Chem.* **2014**, *86*, 514−520.
(30) Sheltami, R. M.; Abdullah, I.; Ahmad, I.; Dufresne, A.; Kargarzadeh, H. Extraction of cellulose nanocrystals from mengkuang leaves (*Pandanus tectorius*). *Carbohydr. Polym.* **2012**, *88*, 772−779.
(31) Johar, N.; Ahmad, I.; Dufresne, A. Extraction, preparation and characterization of cellulose fibres and nanocrystals from rice husk. *Ind. Crops Prod.* **2012**, *37*, 93−99.
(32) Kim, U. J.; Wada, M.; Kuga, S. Solubilization of dialdehyde cellulose by hot water. *Carbohydr. Polym.* **2004**, *56*, 7−10.
(33) Huang, T. C.; Chen, M. H.; Ho, C. T. Effect of phosphate on stability of pyridoxal in the presence of lysine. *J. Agric. Food Chem.* **2001**, *49*, 1559−1563.
(34) Li, H.; Wu, B.; Mu, C.; Lin, W. Concomitant degradation in periodate oxidation of carboxymethyl cellulose. *Carbohydr. Polym.* **2011**, *84*, 881−886.
(35) Iravani, M. R.; Tangestaninejad, S.; Habibi, M. H.; Mirkhani, V. Readily prepared polystyrene-bound pyridine-2,6-dicarboxylate and its application for removal of mercury ions. *J. Iran. Chem. Soc.* **2010**, *7*, 791−798.
(36) Ho, Y. S. Citation review of Lagergren kinetic rate equation on adsorption reactions. *Scientometrics* **2004**, *59*, 171−177.
(37) Ho, Y. S. Review of second-order models for adsorption systems. *J. Hazard. Mater.* **2006**, *136*, 681−689.
(38) Kyzas, G. Z.; Deliyanni, E. A. Mercury(II) removal with modified magnetic chitosan adsorbents. *Molecules* **2013**, *18*, 6193−6214.
(39) Langmuir, I. The constitution and fundamental properties of solids and liquids. *J. Am. Chem. Soc.* **1916**, *38*, 2221−2295.
(40) Ho, Y. S.; Huang, C. T.; Huang, H. W. Equilibrium sorption isotherm for metal ions on tree fern. *Process Biochem.* **2002**, *37*, 1421−1430.

(41) Freundlich, H. M. F. Uber die adsorption in losungen. *Z. Phys. Chem.* **1906**, *57*, 385−470.
(42) Gaspar, D.; Fernandes, S. N.; de Oliveira, A. G.; Fernandes, J. G.; Grey, P.; Pontes, R. V.; Pereira, L.; Martins, R.; Godinho, M. H.; Fortunato, E. Nanocrystalline cellulose applied simultaneously as the gate dielectric and the substrate in flexible field effect transistors. *Nanotechnology* **2014**, *25*, 094008.
(43) Hutchens, S. A.; Benson, R. S.; Evans, B. R.; Rawn, C. J.; O'Neill, H. A resorbable calcium-deficient hydroxyapatite hydrogel composite for osseous regeneration. *Cellulose* **2009**, *16*, 887−898.
(44) Wu, J.; Zheng, Y.; Yang, Z.; Lin, Q.; Qiao, K.; Chen, X.; Peng, Y. Influence of dialdehyde bacterial cellulose with the nonlinear elasticity and topology structure of ECM on cell adhesion and proliferation. *RSC Adv.* **2014**, *4*, 3998−4009.
(45) Chauhan, K.; Chauhan, G. S.; Ahn, J. H. Synthesis and characterization of novel guar gum hydrogels and their use as Cu^{2+} sorbents. *Bioresour. Technol.* **2009**, *100*, 3599−3603.
(46) Ansari, R.; Raofie, F. Removal of mercuric ion from aqueous solutions using sawdust coated by polyaniline. *E-J. Chem.* **2006**, *3*, 35−43.
(47) Eligwe, C. A.; Okolue, N. B.; Nwambu, C. O.; Nwoko, C. I. A. Adsorption thermodynamics and kinetics of mercury(II), cadmium(II) and lead(II) on lignite. *Chem. Eng. Technol.* **1999**, *22*, 45−49.